IET Nanobiotechnology

Research Article

IET Journals
The Institution of Engineering and Technology

Honey-incorporated nanofibre reduces replicative senescence of umbilical cord-derived mesenchymal stem cells

ISSN 1751-8741
Received on 10th September 2019
Revised 15th June 2020
Accepted on 17th August 2020
E-First on 2nd November 2020
doi: 10.1049/iet-nbt.2019.0288
www.ietdl.org

Ankita Das[1], Pallab Datta[1], Amit Roy Chowdhury[1,2], Ananya Barui[1] ✉

[1]*Centre for Healthcare Science and Technology, Indian Institute of Engineering Science and Technology, Shibpur, Howrah 711103, West Bengal, India*

[2]*Department of Aerospace Engineering and Applied Mechanics, Indian Institute of Engineering Science and Technology, Shibpur, Howrah 711103, West Bengal, India*

✉ *E-mail: ananya.pariksha@gmail.com*

Abstract: Umbilical cord-derived mesenchymal stem cells (UCDMSC) are attractive candidates for cell-based regenerative medicine. However, they are susceptible to replicative senescence during repetitive passaging for in-vitro expansion and induced senescence in an oxidative, inflammatory microenvironment in vivo. Aim of this study is to investigate if honey-incorporated matrices can be employed to reduce senescence of UCDMSC. Matrices were prepared by electrospinning solutions of honey with poly-vinyl alcohol (PVA). PVA:honey matrices exhibited free radical scavenging activity. Culture of UCDMSC on PVA:honey matrices showed improvement in cell proliferation compared to pure PVA nanofibres. Expression of vimentin indicated that mesenchymal phenotype is preserved after culturing on these matrices. Further, UCDMSC were serially subcultured and cells of two passages (P2 and P6) were evaluated for reactive oxygen species (ROS) load and senescence parameters. P6 cells showed a higher ROS load and β-galactosidase (β-gal) positive senescent cells compared to P2. However, culturing on PVA:honey substrates significantly reduced both ROS and β-gal markers compared to cells on PVA substrates. Honey contains several antioxidant and anti-inflammatory components, which can reduce the ROS-related senescence. Thus, it is concluded that honey containing nanofibres can be effective substrates for stem cell-based wound healing and regenerative medicine.

1 Introduction

Umbilical cord-derived mesenchymal stem cells (UCDMSC) possess immense potential in tissue engineering and regenerative medicine. In comparison to stem cell obtained from other sources, UCDMSC are ethically compliant repository and have proven potential to differentiate into different cellular lineages like neurons, adipocytes, chondrocytes, hepatocytes, endothelial, epithelial, both in vitro and in vivo [1]. UCDMSC do not elicit strong immunologic reactions due to the presence of low levels of MHC Class-II isotype antigens. However, similar to stem cell from other sources (adult or embryonic), UCDMSC are susceptible to progressive loss of regenerative and differentiation potential due to replicative senescence [2, 3]. Replicative senescence has been identified as one of the major constrains in the clinical translation of stem cells [4]. Under in vitro conditions, repetitive passaging [2], and endogenous reactive oxygen species (ROS) and DNA damage [5] are associated with stem cell senescence. Moreover, the presence of an inflammatory microenvironment both in vitro or in vivo can induce cellular senescence [6]. On the other hand, a hypoxic condition has shown to preserve stem cell integrity in long-term cultures [7]. As senescence is a progressive phenomenon, genetic factors and age of the donor also pre-dispose stem cells harvested for clinical applications to limited ex vivo expansion depending upon the senescence status of harvested cells.

In vitro stem cell expansion by subculturing on tissue culture polystyrene causes cellular biochemical, genetic and epigenetic alterations in cells as well as ROS accumulation with implications on cellular functionalities and senescence [2, 8, 9]. Cellular senescence is associated with characteristic changes in cellular morphology, progressive telomere shortening, cytoskeletal changes and extracellular matrix modification before undergoing permanent growth arrest. One of the key factors identified for such observations is the difference between in vitro and in vivo microenvironment. Natural extracellular matrix is known to provide an assortment of biochemical, biophysical and macromolecular cues to maintain stem cell functionality [10]. Presently, biomaterial strategies are increasingly being explored for efficient expansion, maintenance and directed differentiation of stem cells [11]. Consequently, it becomes imperative that biomaterial-based scalable, cost-effective ex-vivo culturing strategies and stem cell delivery matrices are also developed with potential to provide a micro-environment conducive of reducing senescence of cultured stem cells [12].

To date, interesting results have been reported by Zhou *et al.* [3] who observed that cell-derived extracellular matrix can mitigate hydrogen peroxide-induced senescence in UCDMSC. Senescence-associated β-galactosidase-positive cells were markedly fewer on cell-deposited matrix compared to polystyrene culture plates. Previously, coating tissue culture polystyrene with Wharton Jelly extract has also been shown to reduce the occurrence of replicative senescence in mesenchymal stem cells. The same work also showed that the extract reduces senescence by controlling ROS in subcultured cells [13]. Similar observations on reduction in stem cell senescence have been reported with flavones-loaded nanofibre membranes [14] and resveratrol-doped-polyurethane–polylactide matrices on adipose derived stem cells [15], while chitosan scaffolds have shown similar potential for culture of human foreskin fibroblasts [16]. However, such extract scaffolds pose significant difficulty in scale-up and maintaining cost effectiveness for scaffold fabrication. Therefore, the development of alternative matrices with easily available sources merits investigations.

The regenerative healing potential of honey, a natural material has been effectively employed to fabricate nanofibre matrices with antioxidant and anti-inflammatory properties as scaffolds for wound healing [17]. While the nanofibre architecture provides a favourable surface for cell attachment, honey components can provide the assortment of biochemical cues for maintaining antioxidant and anti-inflammatory microenvironment for cell proliferation. Several components have been identified in honey which provide these necessary functionalities [18]. Considering the bioactive roles of honey-loaded nanofibres, the present study

hypothesised that honey-loaded substrates can reduce senescence during ex-vivo culture of UCDMSCs and it can be developed as delivery matrices in regenerative medicine. Nanofibre substrates are employed for culturing cells after different passage numbers and ROS level and senescence markers of cultured cells are examined.

2 Materials and methods

2.1 Materials

Poly-vinyl alcohol (PVA) with molecular weight – 89–90 kDa was purchased from Sigma Aldrich (USA). Dabur Honey (Lot No. NP4722, Dabur India Limited, Kolkata, India) was purchased from a local market and stored at 4°C. HiMesoXL™ Mesenchymal Stem Cell Expansion Medium (HiMedia, India), antibiotic–antimycotic (100×) (ThermoFisher Scientific, USA), MTT assay kit from HiMedia, India; Live/Dead Double Staining Kit from Merck, USA; DCFDA (2′,7′–dichlorofluorescin diacetate) (DCFDA/H2DCFDA – cellular ROS assay kit from Abcam, USA); senescence histochemical staining kit from G Biosciences, USA and foetal bovine serum from Invitrogen, USA were purchased for cell culture studies. All experiments were performed in triplicate.

2.1.1 Substrate fabrication using electrospinning technique: PVA solution was obtained by dissolving 12 g PVA powder in deionised water (Wasserlab, Spain) by stirring at 80°C. Weighed amounts of honey were added to the PVA solution as 0.2, 0.5 and 1 g. The volume was adjusted to obtain the final concentrations of 12% PVA–0.2% honey (12PH0.2), 12% PVA–0.5% honey (12PH0.5) and 12% PVA–1% honey (12PH1). These concentrations were selected to obtain smooth electrospun nanofibres based on a previous work [19]. Solutions were homogenously stirred at room temperature for 24 h. Nanofibre membranes were prepared by an electrospinning machine (E-SPIN NANOTECH, SUPER ES-1, Kanpur, India). A 5 ml syringe was loaded with different PVA/honey solutions and the voltage was set at 22 kV. The collector to needle distance was kept at 12 cm and the flow rate was set at 0.3 ml/h. The nanofibre membranes were crosslinked with 2 M glutaraldehyde in HCl and acetone for 2 h after electrospinning. All scaffolds were washed thrice with PBS for 10 min at room temperature and dried before sterilising them with UV irradiation for 1 h [20].

2.2 Physico-chemical characterisation

2.2.1 Scanning electron microscopy (SEM): SEM micrographs were captured to visualise the morphology of nanofibres using HITACHI 3400N scanning electron microscope at a voltage of 15 kV. Gold sputter coating was performed on samples before imaging.

2.2.2 Contact angle measurement: Surface tensiometer SURFECTENS 4.5 (OEG GmbH, Germany) was used to evaluate the surface wettabilities of the electrospun membranes for the measurement of water contact angle. The wettability of the nanofibre membranes were determined by dropping distilled water on membrane using the sessile drop technique. The images of the droplets on the scaffolds were visualised using an image analyser. The contact angle was measured ten times from different positions for the different nanofibre membranes and average values are reported.

2.2.3 Antioxidant release study by 2,2-diphenyl-1-picrylhydrazyl hydrate (DPPH) and 2,2′-azino-bis(3-ethylbenzothiazoline-6-sulfonic acid) (ABTS) radical scavenging assay: DPPH assay was used to estimate the PVA–honey nanofibres' radical scavenging activity (RSA). Ethanolic solution of 200 mM DPPH (Sigma Aldrich, USA) was left in dark for 30 min. The nanofibre membranes were placed in PBS for 3 and 5 days, respectively, and the supernatant was incubated with the working solution of DPPH for 30 min at room temperature in dark. Absorbance at 517 nm was measured using UV–Vis spectrophotometer (MultiSkan GO Microplate Spectrophotometer, Thermo Fischer Scientific, Ratastie 2, FI-01620 Vantaa, Finland) and the RSA was calculated using the following formula:

$$\mathrm{RSA}\% = 100 - \left[\left(\mathrm{Abs}_{\mathrm{sample}} - \mathrm{Abs}_{\mathrm{blank}}\right)/\mathrm{Abs}_{\mathrm{control}}\right]$$

where $\mathrm{Abs}_{\mathrm{sample}}$, $\mathrm{Abs}_{\mathrm{blank}}$ and $\mathrm{Abs}_{\mathrm{control}}$ signify the absorbance of the sample, blank and control, respectively, at 517 nm.

Ascorbic acid solution in different concentrations was used as standard. The DPPH assay was performed in triplicates for all the test samples.

A 190 µl of ABTS working solution (7 mM) was added to each of the scaffolds on 96-well plates and incubated for 30 min in dark at 37°C. The absorbance was taken with the help of an UV–Vis spectrophotometer at 734 nm. The same standard was used for this assay. All the experiments were performed in triplicate. The % ABTS RSA was determined by using the formula

$$\text{ABTS radical scavenging activity}\,(\%) = \left(\mathrm{Abs}_{\mathrm{control}} - \mathrm{Abs}_{\mathrm{sample}}\right)/\mathrm{Abs}_{\mathrm{control}}$$

where $\mathrm{Abs}_{\mathrm{control}}$ is the absorbance of ABTS radical in methanol and $\mathrm{Abs}_{\mathrm{sample}}$ is the absorbance of ABTS radical solution mixed with sample.

2.3 Cell culture study

2.3.1 UCDMSC isolation, identification and characterisation: Umbilical cord (UC) was obtained after normal deliveries under informed written consent and approval from the Institutional Ethics Committee of IIEST, Shibpur. UCDMSCs were isolated and cultured according to the protocol described by Mennan *et al.*, 2013, with minor modifications. In brief, UC was washed three times with PBS containing 1% antibiotic solution and 20% betadine (standardised microbiocidal solution, 10%) with gradual reduction in betadine concentration after each wash. UC was then dissected into ∼2–3 cm of length and artery, vein and Wharton's jelly were removed from each section. After mincing the UC into 5–6 mm^3 fragments, samples were incubated with complete HiMeso Stem Cell Expansion Medium (HiMedia, India). Cells were incubated at 37°C, 5% CO_2. After 21 days, the tissue explants were removed. The cells were subcultured upon reaching 60–80% confluency at a density of $1 \times 10^4\ \mathrm{cm}^{-2}$ for further expansion [21].

2.3.2 UCDMSC biomarkers: Isolated cells were stained with positive (CD105) and negative (CD45) markers for identification of UCDMSC. Four percent paraformaldehyde was used to fix the cells for 15 min at room temperature and scaffolds were washed with PBS thrice. Cell suspensions (5×10^5 cells) were incubated with mouse anti-CD105 antibody and mouse anti-CD45 antibody at a dilution of 1:200 (Dako, North America Inc.) overnight in a humidifying chamber at 4°C. Cells were stained with fluorescein isothiocyanate (FITC)-conjugated goat-anti-mouse IgG secondary antibody (1:500) (Santa Cruz Biotechnology, Inc., USA) and incubated at room temperature for 2 h in dark. Immunostained cells were counterstained with 4,6-diamidino-2-phenilindole (DAPI) (Sigma Aldrich, Saint Louis, MO, USA).

2.3.3 Culture of UCDMSC on nanofibres: For biological assays, the nanofibre substrates were seeded with UCDMSC at a concentration of 5×10^4 cells/ml and cultured in as described for each experiment.

2.3.4 MTT cell viability test: The viability of cells cultured on nanofibres was assessed through MTT assay (EZcount™ MTT cell Assay Kit, HiMedia, Mumbai, India). UCDMSC were trypsinised and suspended in 100 µl of HiMeso mesenchymal stem cell expansion medium/well at a final concentration of 5×10^4 cells/well and cultured in 96-well plate. After 3 days incubation, MTT solution was added to each well along with serum-free cell culture

media. Cells were incubated for another 4 h at 37°C and 100 µl of solubilisation buffer was added to the well plates and were put on a shaker for 10 min. Then, the nanofibre membranes were taken out and 100 µl of the supernatant from each test group was pipetted into a fresh 96-well plate. The optical density at 570 and 670 nm was measured using an UV–Vis multi-plate spectrophotometer (Thermo Scientific™ Multiskan™ GO Microplate Spectrophotometer, Finland). Same procedure was repeated by culturing cells on the nanofibre membranes for 5 days for estimating the cell viability. Percentage of cell viability was calculated by the following formula:

$$\%\ \text{cell viability} = [(\text{Abs}_{\text{test}} - \text{Abs}_{\text{blank}})/\text{Abs}_{\text{control}} - \text{Abs}_{\text{blank}}] \times 100$$

where Abs_{test}, $\text{Abs}_{\text{blank}}$ and $\text{Abs}_{\text{control}}$ signify the absorbance of the sample, blank and control, respectively, at 570 nm.

2.3.5 Live/dead cell viability test: Cells cultured on nanofibre membrane for 5 days were stained with the 100 µl staining solution and incubated for 15 min at 37°C according to manufacturer's protocol (QIA76 Live/Dead Double Staining kit, Merck, India). After incubation, cells were analysed under a fluorescence microscope (Nikon eclipse Tí U, Japan).

2.3.6 Expression of vimentin and CD105: Cells cultured on nanofibre membranes after 5 days were fixed with 4% paraformaldehyde for 15 min and permeabilised with 0.1% Triton X-100 at room temperature. Cells were incubated with anti-vimentin primary antibody (1:200) (MAB3400, Merck, India) and mouse anti-CD105 antibody (1:200) (Dako, North America Inc.) overnight at 4°C after blocking with 1% bovine serum albumin (BSA) in PBS. After thorough washing, cells were incubated with goat anti-rabbit IgG conjugated with FITC (1:200) (Santa Cruz Technology, Shanghai) secondary antibody for 2 h at room temperature. Immunostained cells were counterstained with DAPI (Sigma Aldrich, Saint Louis, MO, USA). Mounting media (Sigma Aldrich) was used to mount the cells on the slide after thorough washing of the cells with 1X PBS.

2.3.7 Phalloidin staining: After culturing for 5 days, nanofibre-cell constructs were washed in PBS (pH 7.4) and fixed in 4% paraformaldehyde for 15 min. After washing with PBS, constructs were incubated with 50 µg/ml rhodamine-conjugated phalloidin (Invitrogen, CA, USA) for 90 min and counterstained with 1 µg/ml of DAPI for 1 min.

2.3.8 Measurement of ROS by DCFDA staining and nitro blue tetrazolium chloride (NBT) assay: ROS production of cells ($P = 2$ and $P = 6$) cultured on nanofibre membranes were assessed with DCFDA (DCFDA/H2DCFDA – cellular ROS detection assay kit). UCDMSC seeded on scaffolds were cultured at passage 2 (P2) and passage 6 (P6) for 5 days. The media were discarded and washed with 1X PBS. Cell-seeded substrates were incubated with incomplete media and DCFDA at a concentration of 20 µM for 30 min at 37°C and 5% CO_2 in dark condition. Cells were finally washed with PBS before image acquisition.

NBT (nitro BT) (extrapure AR, 99%) at a concentration of 0.1 mg/ml in 1× PBS was used as working solution. For assay, UCDMSC cultured on PVA:honey nanofibre membranes was trypsinised and incubated with 300 µl of the working solution for 15 min at room temperature. The cells were washed thoroughly with 1× PBS and the formazan crystals that were formed were dissolved by adding 300 µl DMSO. A 100 µl of the dissolved solution from each test group was aliquot in 96-well plate and the measurement was taken at 630 nm using an UV–Vis multi-plate spectrophotometer (Thermo Scientific™ Multiskan™ GO Microplate Spectrophotometer, Finland).

For differential interference contrast (DIC) and fluorescence microscopy, images were acquired through inverted fluorescence microscope (Nikon eclipse Tí U, Japan) equipped with 20× objective. Fluorescence intensity of the images was measured using ImageJ software (version 1.44p). For intensity estimation in ROS, the green fluorescent intensity of cells was calculated from five field of views (FOVs). For each study groups, ∼75 cells were considered for the analysis. The fluorescence intensity of individual cell was calculated and averaged for each image frame using imageJ software (version 1.44p). Representative DIC/fluorescence merged images were obtained with the help of NIS-Elements software [22, 23].

2.3.9 Senescence-associated β-galactosidase staining for senescence detection: UCDMSC cultured on PVA and honey-loaded nanofibre substrates at $P = 2$ and $P = 6$ were fixed with 1× fixing solution provided in the kit for 10 min at room temperature. About 200 µl of staining solution (senescence histochemical staining kit, G-Biosciences, USA) was added to each well according to manufacturer's protocol. The well plates were incubated at 37°C for 12 h.

For β-gal study, cell imaging was performed through bright-field mode using 20× objective. Total number of positively stained cells (blue) was counted from ∼60 cells from each study group using ImageJ software. The percentages of positively stained cell were estimated by using the formula: % of β-gal positive cells = total number of blue cells (β-gal positive)/total number of cells (number of β-gal positive cells + number of β-gal negative cells) × 100 [24, 25].

2.3.10 Determination of senescence associated secretory phenotype cytokine, IL-6 by immunocytochemistry: UCDMSC cultured on nanofibre membranes after 5 days were fixed with 4% paraformaldehyde for 15 min and permeabilised with 0.1% Triton X-100 at room temperature. Cells were incubated with mouse anti-IL-6 primary antibody (1:22) (4 µg/ml) in 1% BSA in PBST (Developmental Studies Hybridoma Bank, Iowa, USA) for 2 h at room temperature After thorough washing, cells were incubated with goat anti-rabbit IgG conjugated with FITC (1:200) (Santa Cruz Technology, Shanghai) secondary antibody for 2 h at room temperature. Immunostained cells were counterstained with DAPI (Sigma Aldrich, Saint Louis, MO, USA). Mounting media (Sigma Aldrich) were used to mount the cells on the slide after thorough washing of the cells with 1× PBS.

2.4 Image acquisition

For fluorescence microscopy, images were acquired through inverted fluorescence microscope (Nikon eclipse Tí U, Japan) equipped with 20× objective. Three different fluorescence filters (λ_{ex}340–380 nm and λ_{em}435–485 nm, λ_{ex}465–495 nm and λ_{em}515–555 nm, λ_{ex}512–552 nm and λ_{em}565–615 nm for blue, green and red emission, respectively) were used for imaging. Fluorescence intensity of the images was measured using ImageJ software (version 1.44p). For β-gal study, cell imaging was performed through bright-field mode using 20× objective. For intensity estimation for vimentin, ROS and IL6 expression, five FOVs consisting of five to six cells were selected from each study groups and each experiment was performed in triplicate. The fluorescence intensity of individual cell was calculated and averaged for each image frame using ImageJ software (version 1.44p). The dimension of fluorescence and bright field images are 1280 × 1024 and 2560 × 1920 pixel, respectively.

2.5 Statistical analysis

All values are expressed as mean±standard deviation of at least three experiments for each batch of PVA–honey nanofibre membrane using one-way ANOVA with Dunnett post-hoc test. Comparison between different experimental groups was performed. Values of $p < 0.05$ and $p < 0.0001$ were considered to be statistically significant. The significance value was calculated by using Prism 5.04, Graphpad Software, CA, USA [26].

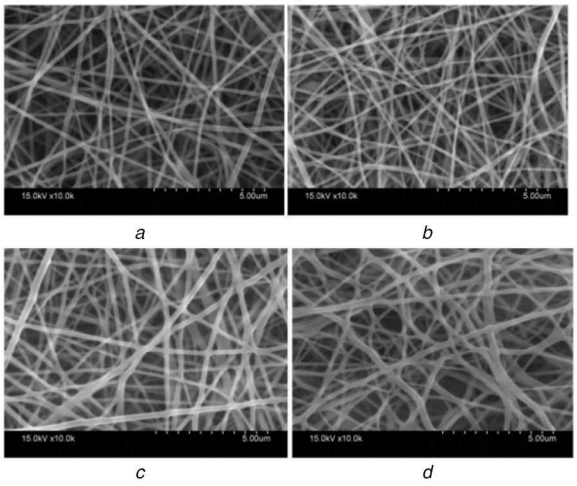

Fig. 1 *SEM images of electrospun nanofibres*
(a) 12PH0, ***(b)*** 12PH0.2, ***(c)*** 12PH0.5, ***(d)*** 12PH1 at 10,000× magnification

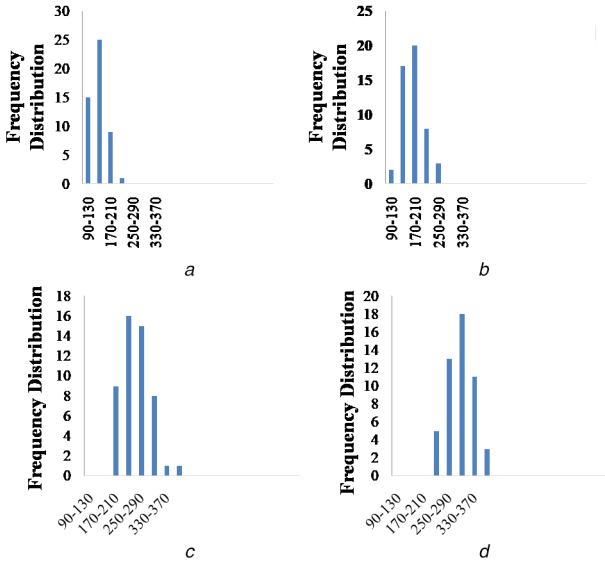

Fig. 2 *Frequency distribution histogram plot for nanofibre diameters of*
(a) 12PH0, ***(b)*** 12PH0.2, ***(c)*** 12PH0.5, ***(d)*** 12PH1

3 Results

3.1 Physico-chemical characterisation of nanofibres membranes

Surface morphology of the nanofibre matrices (Figs. 1*a–d*) showed formation of uniform, bead-free nanofibres for all the combinations evaluated.

It was also evident that honey incorporation increased the diameter of the nanofibres. The diameter of nanofibres was 144 ± 27, 184 ± 36, 255 ± 44 and 305 ± 43 nm for 12PVA, 12PH0.2, 12PH0.5 and 12PH1, respectively, as depicted in the frequency distribution graph (Figs. 2*a–d*). Detailed analysis of nanofibre dimension was measured from the SEM images with ImageJ software. Approximately 200 fibre strands were analysed for each study group.

These observations corroborated with previous reports where increase in fibre dimensions due to honey incorporation has been attributed to increase in viscosity and hygroscopicity of the nanofibres. Previous studies have also reported that PVA-based nanofibre substrates with similar characteristic are ideal for cell culture [27]. Further, honey incorporation in PVA nanofibres also increased the hydrophilic character of the matrices as the measured water contact angles decreased to 52°, 47° and 46° for 12PH0.2, 12PH0.5 and 12PH1, respectively, from 57° measured for pure PVA nanofibre matrices (Fig. 3). Generally, it is assumed that increased hydrophilicity improves the attachment of stem cells [28]. In the present study, hydrophilic behaviour of membranes is

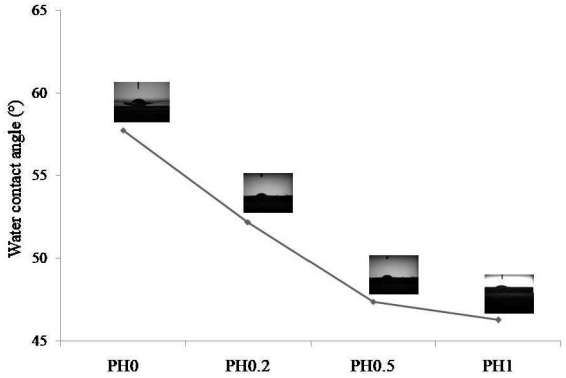

Fig. 3 *Graphical representation of water contact angle of 12PH0, 12PH0.2, 12PH0.5 and 12PH1 nanofiber membranes*

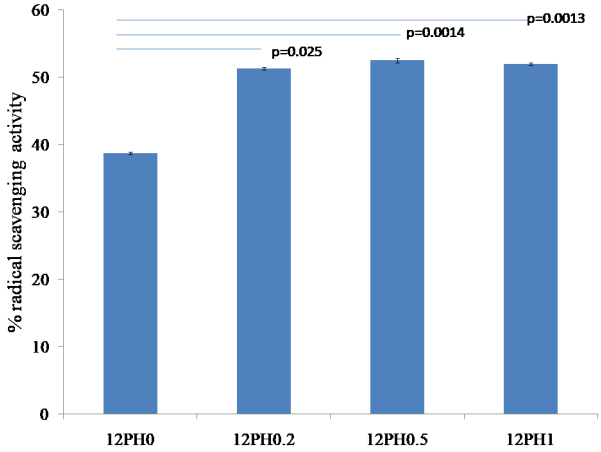

Fig. 4 *Antioxidant release from PVA–honey nanofibre membranes measured by DPPH radical scavenging assay showing the optimum antioxidant activity provided by 12PH0.5 compared to the other nanofibre membrane groups*

later corroborated with the adhesion and proliferation of UCDMSC.

3.2 Antioxidant property of the nanofibre membranes

The DPPH reagent shows absorbance at 517 nm wavelength and contains stable free radicals, which are scavenged by antioxidants released from the nanofibre membranes, therefore providing quantitative information on antioxidant property. As shown in Fig. 4, the PVA nanofibre showed 38% RSA. The scavenging activity was significantly increased in 12PH0.2 (51.3%) and further in 12PH0.5 (52.5%). However, no significant difference was found between 12PH0.5 and 12PH1 (51.4%). The RSA of honey is defined by antioxidant phenolic contents such as benzoic acid, cinnamic acid and their ester derivatives [29]. However, honey also contains pro-oxidants like H_2O_2 and low concentrations of honey are known to produce low hydrogen peroxide levels and therefore, a balance level between antioxidants and pro-oxidants are observed [30]. Several other investigators have also found optimal honey concentrations for antioxidant activities in both raw honey dilutions and scaffold forms [31]. Similar trend was observed in ABTS assay as shown in Fig. 5.

3.3 Characteristics of isolated UCDMSC

Isolated UCDMSC showed alteration in morphology after few days of culture compared to morphology obtained in immediately after isolation. Cells first attached on day 6 of isolation and assumed polygonal, spindle and spread-out morphologies gradually. Isolated cells showed positive expression of CD105 and negative expression for CD45 (Fig. 6). It confirms the stemness of the isolated cells obtained from UC [32].

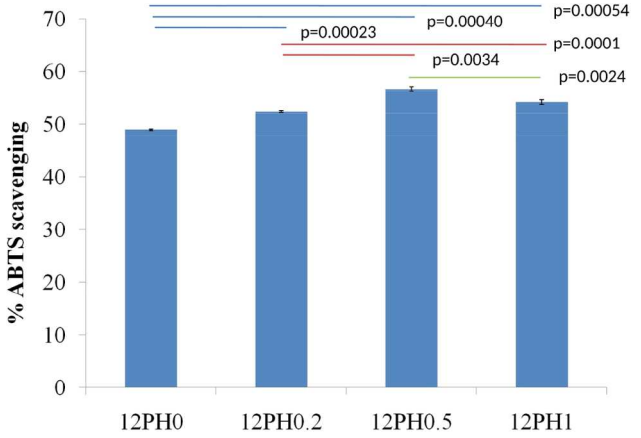

Fig. 5 *Antioxidant release from PVA-honey nanofiber membranes measured by ABTS radical scavenging assay shows the optimum antioxidant activity provided by 12PH0.5 compared to the other nanofiber membrane groups. The experiment was performed in triplicate*

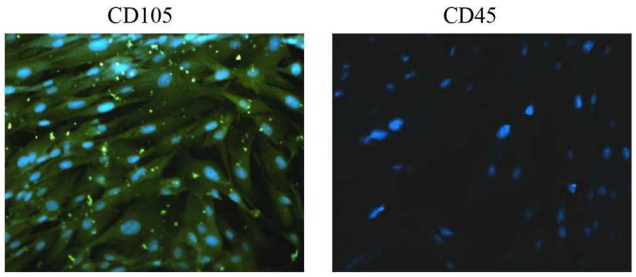

Fig. 6 *Expression of positive (CD105) and negative (CD45) markers on isolated MSCs*

3.4 Cell viability assay

MTT assay results were further confirmed by live/dead assay as represented in Fig. 7*b*. In all the substrates, number of live cells was greater than dead cells, though the proportion of live to dead cells increased along with increased honey concentration of the substrates, i.e. 63, 74, 87 and 83% in 12PH0, 12PH0.2, 12PH0.5 and 12PH1, respectively.

To evaluate the cytocompatibility of matrices with stem cells, viability of UCDMSC cultured on nanofibre membranes was studied through MTT assay (Fig. 7*a*) after 3 and 5 days of culture. The cellular viability in control group was considered as 100%. The highest cell viability was observed in 12PH0.5 with ∼117 and ∼128% for 3 and 5 days, respectively. On the other hand, 12PH0 showed the lowest viability of UCDMSC for both 3 days (∼75%) and 5 days (∼93%) of culture. A significant increase in cellular viability was observed between honey-containing membranes and pure PVA membrane after 5 days of culture. However, in between 12PH0.5 and 12PH1, no significant change in cellular activity was observed. Result indicates that honey incorporation in scaffolds improved the compatibility of nanofibre substrates of PVA with UCDMSC, as is seen with other cell types like fibroblasts and osteoblasts [27, 33]. However, this is the first study on interaction of honey-based substrates with any type of mesenchymal stem cells.

3.5 Cytoskeleton arrangement

Phalloidin staining (Figs. 8*a–d*) showed the distribution of actin filament of attached UCDMSC on different substrates.

3.6 Vimentin and CD105 expression

After ensuring the non-cytotoxic nature of the honey-incorporated nanofibres, the ability of nanofibres to maintain the integrity of UCDMSC was evaluated by quantifying the expression of vimentin. Vimentin is an intermediate filament (IF) protein expressed in mesenchymal stem cells [34]. The expression of

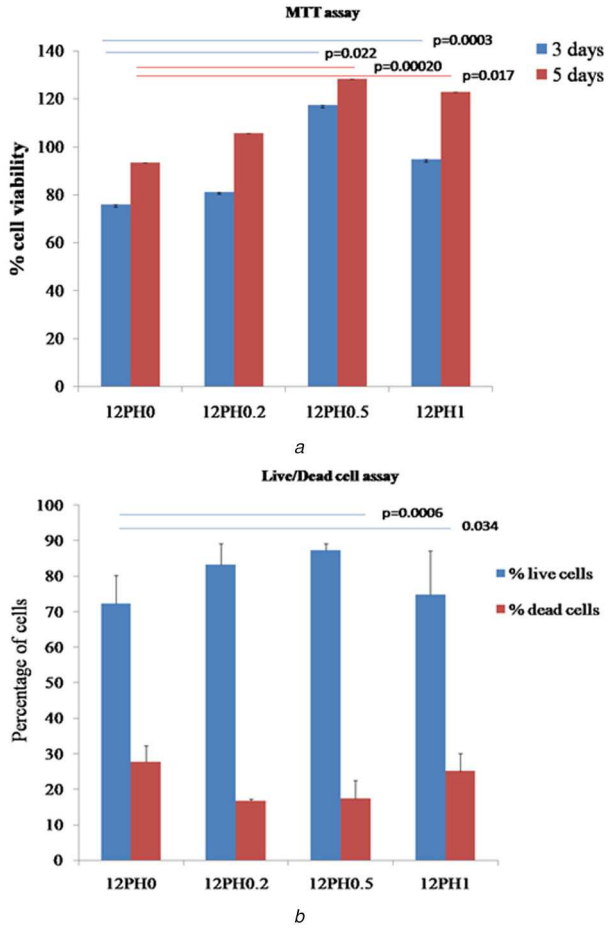

Fig. 7 *Representing the viability of UCDSMSC on different nanofibre membranes at 3 and 5 days of culture by*
(a) MTT assay, ***(b)*** Live/dead double staining assay

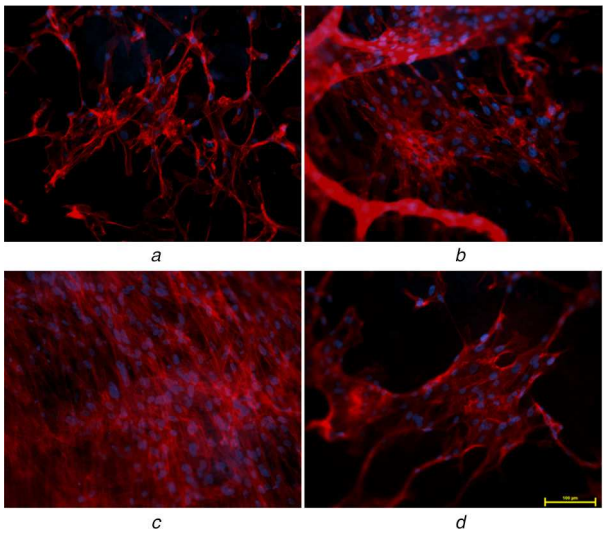

Fig. 8 *F-actin filaments showing cytoskeletal network of UCDMSC cultured on different PVA–honey nanofibre membranes*
(a) 12PH0, ***(b)*** 12PH0.2, ***(c)*** 12PH0.5, ***(d)*** 12PH1

vimentin is higher in undifferentiated stem cells whereas expression of this marker is markedly reduced as cells fate change towards differentiated lineages [35].

Researchers have identified four markers, CD29, CD44, CD105 and vimentin, strongly expressed in undifferentiated mesenchymal stem cells [36, 37]. In the present study, the expression of vimentin (green) (Fig. 9*a*) in 12PH0 is visibly less in comparison to PVA–honey nanofibres (Figs. 9*b–d*). Quantitative analysis of the expression (Fig. 10) further revealed that the intensity was lowest in 12PH0 (∼40 arbitrary unit, i.e. au) which significantly increased

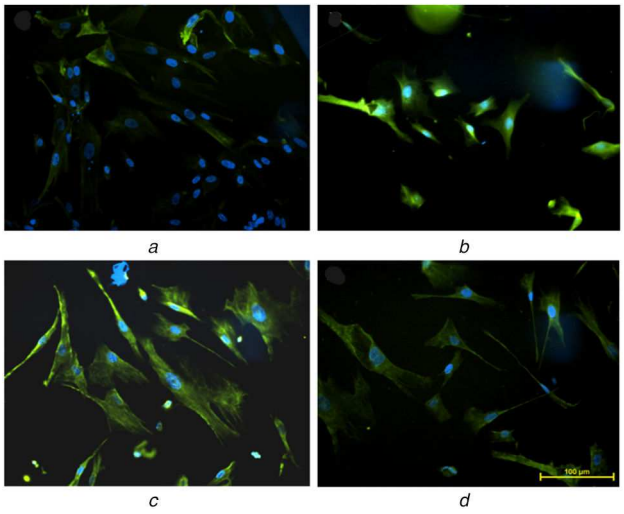

Fig. 9 *Expression of vimentin in UCDSMSC cultured on* ***(a)*** 12PH0, ***(b)*** 12PH0.2, ***(c)*** 12PH0.5, ***(d)*** 12PH1

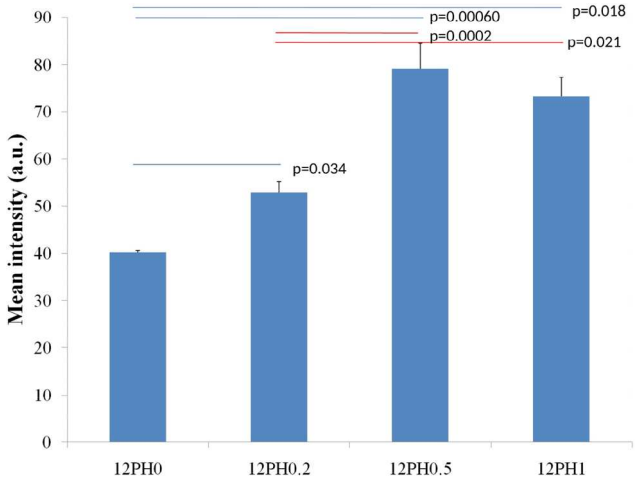

Fig. 10 *Intensity distribution of vimentin in different study groups*

in PH0.2 (~50 au), PH0.5 (~79 au) and PH1 (~80 au). UCDMSC showed similar expression trend with CD105 on the different nanofibre membranes as shown in Figs. 11 and 12.

It becomes evident that honey matrices help in maintenance of the stemness of UCDMSC. Further, expression of vimentin also has a correlation with the cellular ROS. Generally with prolonged culture, increase in cell membrane ROS concentration in culture media is enhanced, which can induce stem cell differentiation into certain lineages [38]. It is observed that vimentin expression significantly reduces in the presence of oxidative agents [9]. In addition, ROS accumulation causes vimentin to be replaced by other IF which initiate cellular differentiation [39].

3.7 ROS production

For application in clinical regenerative medicine, UCDMSC are required at large numbers for which serial passaging is essential. However, increase in each passage number invariably results in loss of cell viability, stem-cell properties and driving the cells towards senescence [40]. Accumulation of increased ROS loads has been identified to be one of the factors leading to stem cell ageing and death. The relationship between ROS production with proliferation of stem cells is also well established [41]. ROS are generated due to activity of mitochondrial complexes and lower ROS level facilitates cellular proliferation and differentiation [42]. However, higher concentration of these free radicals induces damage in important biomolecules including DNA, proteins and lipids as well as causes cellular dysfunction, induction of senescence [43] or aberrant differentiation. In a study by Estrada *et al.* [44], it has been demonstrated that ROS-induced senescence of

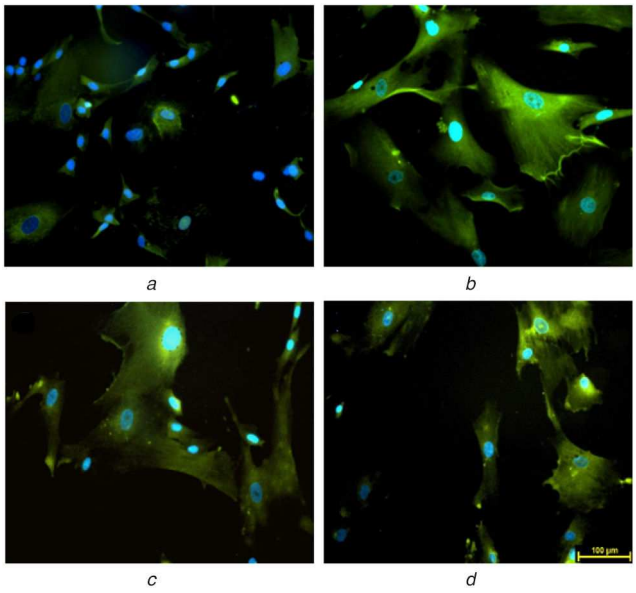

Fig. 11 *Expression of CD-105 in serially subcultured cells at P2 on* ***(a)*** 12PH0, ***(b)*** 12PH0.2, ***(c)*** 12PH0.5, ***(d)*** 12PH1

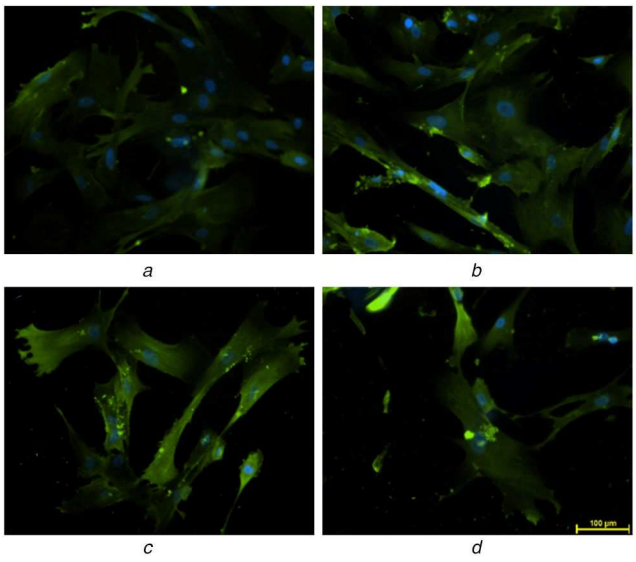

Fig. 12 *Expression of CD-105 in serially subcultured cells at P6 on* ***(a)*** 12PH0, ***(b)*** 12PH0.2, ***(c)*** 12PH0.5, ***(d)*** 12PH1

UCDMSC originates exclusively from mitochondria, observed with enhanced mitochondrial oxygen consumption rate with increase in passage numbers of stem cells.

In the present study, the effect of honey incorporation in the nanofibres on ROS mitigation of stem cells at different cellular passage numbers ($P = 2$ and 6) was examined and is represented in Figs. 13 and 14. Higher accumulation of ROS was observed in UCDMSC in P6 in comparison to P2 in all study groups (Fig. 14). The intensity analysis (Fig. 15) for ROS at P2 showed ROS accumulation decreased with incorporation of honey. In P2, the PVA substrates showed average ROS intensity of ~18.9 au whereas with incorporation of honey the ROS accumulation was significantly ($p < 0.05$) decreased.

Nanofibre membranes of 12PH0.2, 12PH 0.5 and 12PH1 showed intensity values of ~17.29, 16.8 and 18.6 au, respectively. Although the difference in ROS intensity value between PVA and honey containing substrates were statistically significant, among honey containing nanofibres, no significant difference in ROS was observed at P2. While comparing the ROS accumulation at P2 and P6, the higher ROS was observed at P6 in comparison to P2 for all the study groups. The difference between ROS intensity values at P2 and P6 was highest in 12PH0 nanofibres and was significant (~18.9 and 21.8 au, respectively). For 12PH0.2 and 12PH1, the

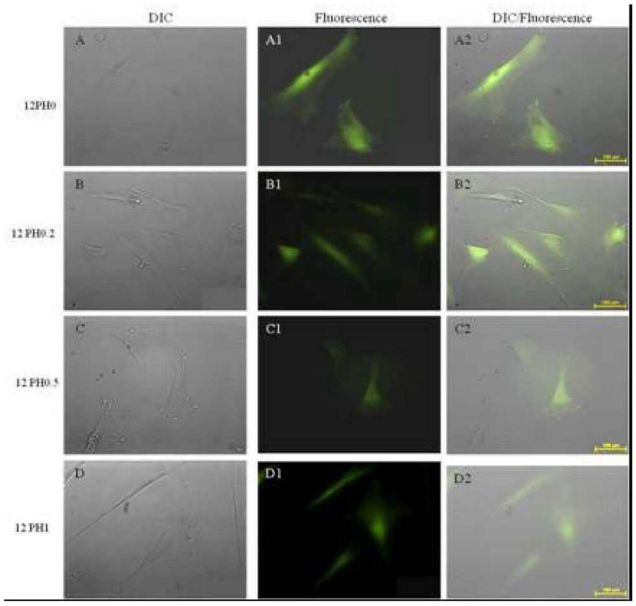

Fig. 13 *Expression of endogenous ROS load in serially subcultured cells at P2 on 12PH0 (A, A1, A2), 12PH0.2 (B, B1, B2), 12PH0.5 (C, C1, C2) and 12PH1 (D, D1, D2) as represented by DIC, fluorescence and DIC/ fluorescence merged images, respectively*

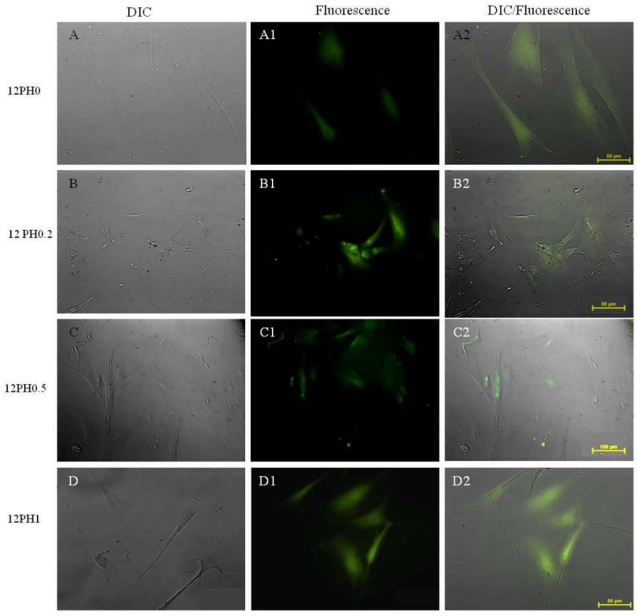

Fig. 14 *Expression of endogenous ROS load in serially subcultured cells at P6 on 12PH0 (A, A1, A2), 12PH0.2 (B, B1, B2), 12PH0.5(C, C1, C2) and 12PH1 (D, D1, D2) as represented by DIC, fluorescence and DIC/ fluorescence merged images, respectively. Scale bar: 100 μm*

ROS level was significantly ($p < 0.05$) increased at P6 though the difference between ROS at P2 and P6 was not significantly different in 12PH0.5. Moreover, the ROS intensities in 12PH0.5 and 12PH1 were significantly lower in comparison to 12PH0.2 for both the passages. In 12PH0.5, the ROS intensity was lowest and its difference with PH1 group was not significant.

A similar trend was observed when NBT assay was performed as shown in Fig. 16. This indicates that probably a higher ROS has been generated due to high proliferation activity on the different nanofibre membranes. The ROS level is effectively reduced by culturing cells on 12PH0.5 nanofibres, suggesting that concentration optimisation with respect to biological properties may drive better selection of materials (Fig. 17).

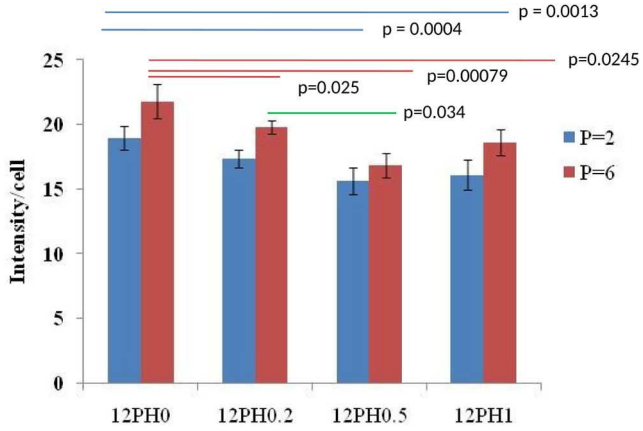

Fig. 15 *Intensity graph representing ROS accumulation on 12PH0, 12PH0.2, 12PH0.5 and 12PH1 at P2 and P6*

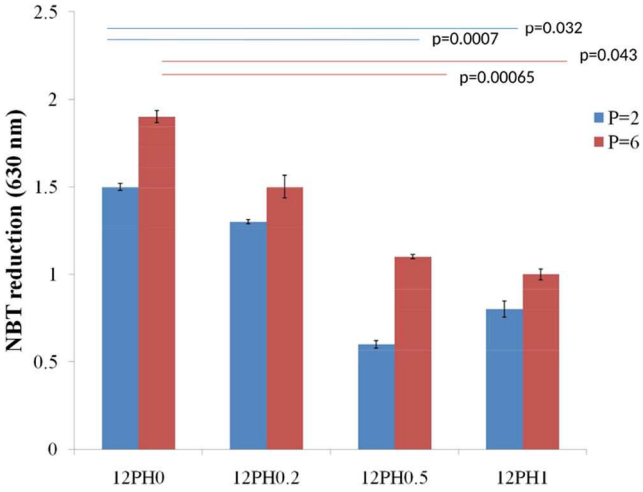

Fig. 16 *Quantification of ROS using a colorimetric NBT assay. ROS generation by cells from different nanofiber membranes was measured by using the colorimetric NBT assay done in triplicate set. Graphical representation shows there is significant decrease in ROS generation in cells cultured on 12PH0.5 and 12PH1 as compared to control*

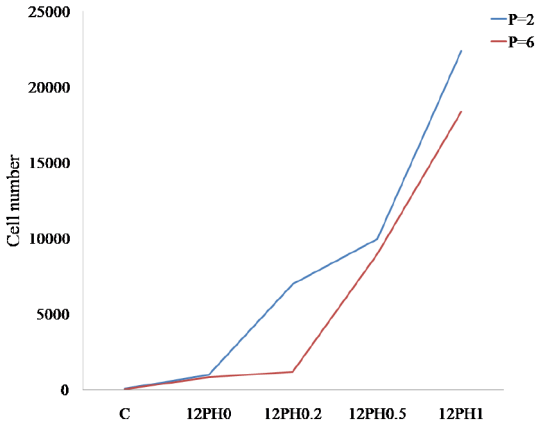

Fig. 17 *Proliferative potential of MSCs at P2 and P6*

3.8 Senescence-associated β-gal staining

On examination of reducing ROS load of UCDMSC by honey containing substrates, their ability to affect senescence was evaluated. β-gal is an important marker associated with senescence of mesenchymal stem cells. Research has showed that loss of β-gal and gain of vimentin delayed the senescence onset on cultured stem cells [24]. Similar to the intensity value for ROS, the β-gal expressions in cultured cells were increased from P2 to P6 (Figs. 18 and 19).

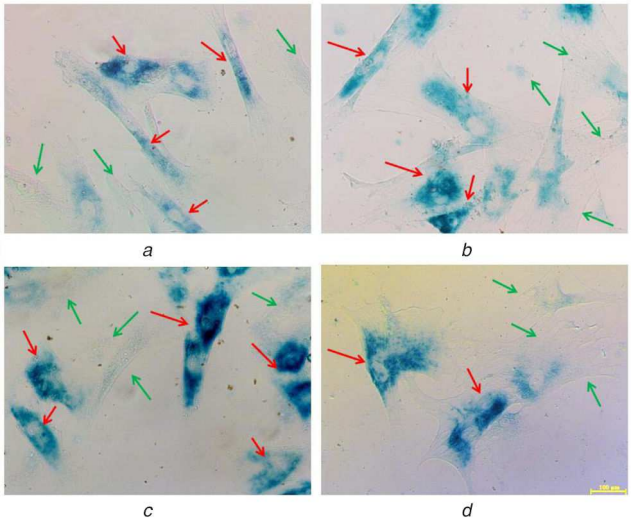

Fig. 18 *Expression of β-gal positive cells cultured on different nanofibre membranes*

(a) 12PH0, ***(b)*** 12PH0.2, ***(c)*** 12PH0.5, (***d)*** 12PH1 at P2. The red and green arrows indicate the expression of β-gal positive and negative cells

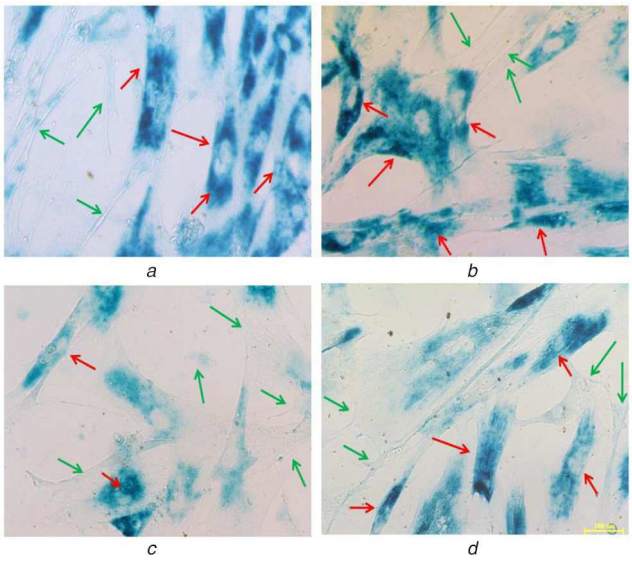

Fig. 19 *Expression of β-gal positive cells cultured on different nanofibre membranes*

(a) 12PH0, ***(b)*** 12PH0.2, ***(c)*** 12PH0.5, ***(d)*** 12PH1 at P6. The red and green arrows indicate the expression of β-gal positive and negative cells

At P2, the number of β-gal positive cells was visibly lower in honey incorporated substrates in comparison to pure PVA fibres (Figs. 18*a–d*). The percentage of β-gal positive cells is lowest in 12PH0.5 in comparison to 12PH0 and 12PH0.2. However, there is no significant difference in percentage between 12PH0.5 and 12PH1 for P2. For P6 (Figs. 19*a–d*), the number of positively stained cells was increased in all study groups. The percentage (Fig. 20) of β-gal positive cells was measured for all study groups at both P2 and P6.

It was observed that percentage of β-gal positive cells was highest in cells cultured on PVA nanofibres (59 and 74 au). For P2 and P6, with increasing honey concentration in membrane, the percentage of β-gal positive cells significantly reduced. At P6, the percentage of β-gal positive cells was significantly reduced in 12PH0.5 in comparison to 12PH0 and 12PH0.2. It was also observed that intensity of IL-6 was highest in cells cultured on 12PH0 and for P2 and P6, with increasing honey concentration in the nanofibre membrane, IL-6 showed decreased expression (Figs. 21 and 22). At P6, intensity of IL-6 was significantly reduced in 12PH0.5 in comparison to 12PH0 and 12PH0.2

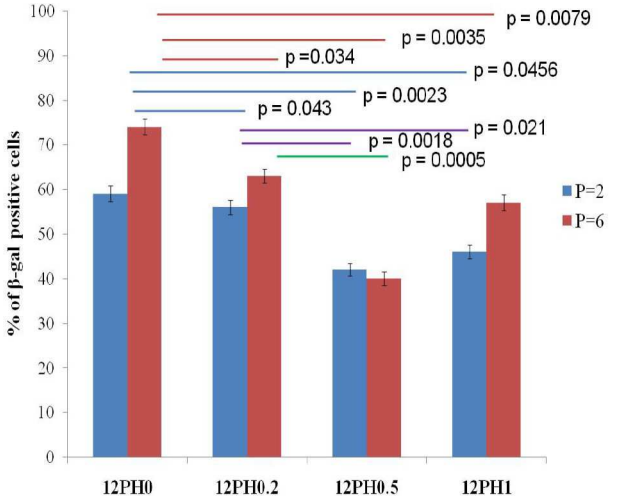

Fig. 20 *Percentage of β-gal positive cells cultured on different study groups at P2 and P6 passages*

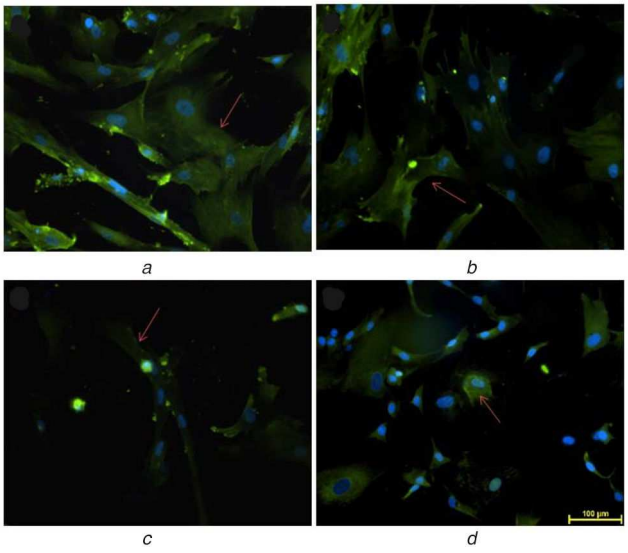

Fig. 21 *Expression of IL-6 in UCDSMSC cultured at P2 on*

(a) 12PH0, ***(b)*** 12PH0.2, ***(c)*** 12PH0.5, ***(d)*** 12PH1. The red arrows indicate the expression of IL-6

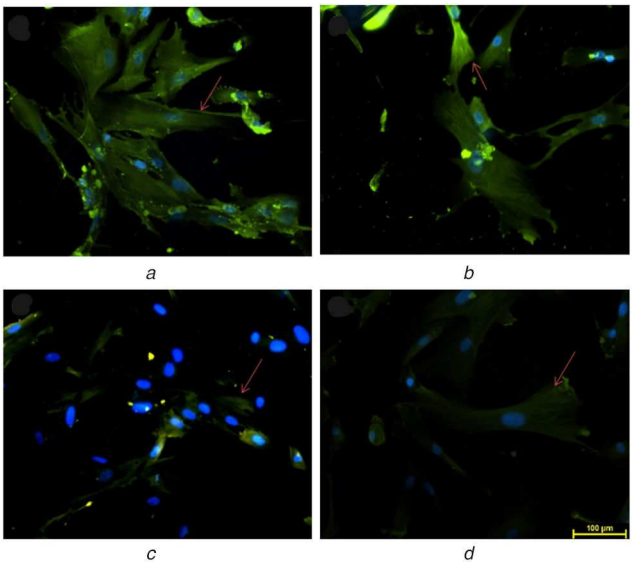

Fig. 22 *Expression of IL-6 in UCDSMSC cultured at P6 on*

(a) 12PH0, ***(b)*** 12PH0.2, ***(c)*** 12PH0.5, ***(d)*** 12PH1. The red arrows indicate the expression of IL-6

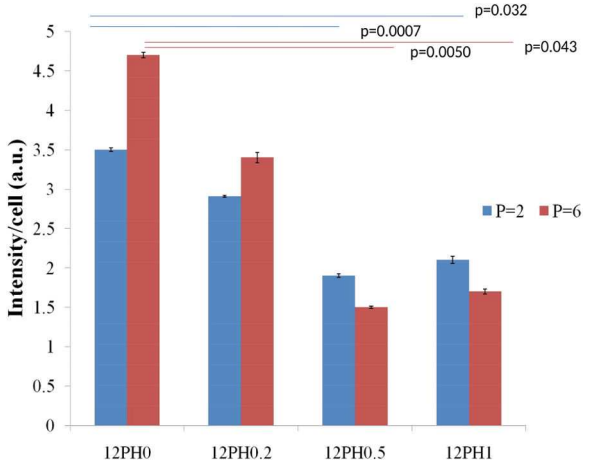

Fig. 23 *Intensity graph of IL-6 on different study groups at P2 and P6 passages*

following similar trend as estimated by showing β-gal activity (Fig. 23).

4 Discussion

Honey is a biologic wound dressing with documented efficacy in traditional literature as well as in modern clinical applications [45]. Recently, the antibacterial properties of Manuka honey against antibiotic resistant strains of bacteria have attracted attention in biomaterial scaffold fabrication for bone regeneration [31]. Such activity has been ascribed to the presence of methylglyoxal content through a non-peroxide mediated mechanism [46]. Similarly, the antioxidant and anti-inflammatory components of honey have found extensive investigation in biomaterial application [47]. On the other hand, senescence of stem cells has remained as the principal mechanism undermining their long-term expansion and in vivo delivery for clinical applications. Senescence in stem cells accrues due to serial sub-culturing. The role of oxidative stress accumulation in determining such cellular response has been elucidated [48]. To evaluate the extent of replicative senescence, cells can be stained by senescence-associated β-gal. Although a basal level of oxidative stress is present in every cell, they become compromised when the physiological balance between oxidant and antioxidant species gets perturbed giving rise to a high level of ROS within the cell. Superoxide radicals and hydrogen peroxide are important ROS having identified the role in the augmentation of ageing and related diseases [49, 50]. The action of antioxidant enzymes decreases with age and homeostasis, which otherwise maintains the balance between pro-oxidants and antioxidants resulting in increased expression of ROS [51].

Mitochondrial pathways are known to contribute to priming the senescence process, through the alteration of mitochondrial redox state [52, 53]. In recent years, natural antioxidants have been explored extensively for regulating cellular behaviour. Polyphenols are the most abundant antioxidants having redox properties. Free radicals such as hydrogen donors, singlet oxygen quenchers, metal chelators and reductants of ferryl haemoglobin are scavenged by polyphenols [54]. Honey, in this context offers a promising proposition to reduce cellular senescence by release of different flavonoids and polyphenols from the fabricated substrates [55]. Therefore, it was of interest to see if honey-based substrates can be fabricated to reduce senescence of stem cells. Moreover, after in-vivo implantation, inflammatory mediators also act to induce senescence of stem cells and the various anti-inflammatory components of honey are expected to provide complimentary support.

In a previous work, PVA–honey electrospun nanofibre matrices were fabricated with different honey concentrations as anti-inflammatory matrices for wound healing. The same compositions were selected as PVA is one of the most conveniently electro-spinnable polymers and allows incorporation of low levels of honey in beads free nano-fibre matrices. Secondly, PVA matrices are inherently inert to most of the cells and hence can act as a suitable substrate for investigating the role of additives. Honey–PVA nanofibres in the range of 180–300 nm were fabricated, a dimension range which approximates other PVA–honey nanofibre mats are reported in the literature [19]. UCDMSC were isolated by maintaining the standard protocol. In our work, it was found that the cells were of rounded morphology until they adhered on the tissue culture flask at day 6, after which the cells gradually get transformed to elongated shape. After day 21, as the cells reached confluency, the explants were removed from the flasks. The isolation of mesenchymal stem cell was confirmed by performing immunocytochemistry and detecting the expression of positive mesenchymal stem cell marker CD105 and absence of negative mesenchymal stem cell marker CD45. Leveraging the traditional knowledge of honey in wound healing, several studies have already shown the biocompatibility of honey nanofibres with keratinocytes and osteoblasts [31]. All studies have concluded that honey incorporation can significantly improve cell compatibility of scaffolds. However, compatibility of honey scaffolds with stem cells and their proliferation behaviour was not known. Therefore, viability and proliferation behaviour of UCDMSC was investigated by an MTT assay and visualised by live/dead staining assay while their cytoskeletal morphology was ascertained by phalloidin rhodamine staining. It was evident that honey-based substrates promoted cell growth over the inert PVA matrices. We observed that 0.5 or 1% honey incorporation significantly increases cell proliferation compared to a 0.2% honey substrate which corroborating with the study by Hixon *et al.* [55], which showed increased viability of MG63 cells cultured on honey-biomaterial matrices containing 1–10% honey. Moreover, the ability of the matrix to preserve mesenchymal phenotype was confirmed by vimentin staining.

The maintenance of the cellular status of UCDMSC has direct implications on their therapeutic usefulness. Estimation of ROS load in the UCDMSC when cultured on these nanofibre substrates was the first functional test performed in a passage-dependent manner as it is well known that cells cannot grow indefinitely and undergo the Hayflick phenomenon induced by replicative senescence. A decrease in the ROS load of cells by culture on poly(ethylene glycol)-polcaprolactone matrices has been reported by Balikov *et al.* [56]. Similarly, our study hypothesised that the passage-dependent ROS load increase in cells can be reduced by culturing UCDMSC on antioxidant PVA:honey nanofibre substrates. Previously, Tan *et al.* [57] have found that culturing corneal progenitor cells with 0.0004–0.4% of Tulang honey reduces oxidative stress of cells. Their results have also shown that concentrations of honey as media supplement above 3.33% may be toxic to the cells. Moreover, the balancing act of pro-oxidant and antioxidant components of honey in reducing cellular stress was also evident from their study. The senescent status of the UCDMSC cultivated on nanofibre substrates in this study at both early ($P = 2$) and late stages ($P = 6$) was confirmed by the decreased activity of endosomal β-D-galactosidase. Interestingly, both ROS load and senescent positive cells were lower in P6 cultured on 12PH0.5 compared to P2 cells cultured on 12PVA, suggesting significant recovery of cellular damage mediated by ROS.

Though the underlying molecular mechanisms associated with replicative senescence are not yet extricated in details, it is known to have consequences for stem cell therapy [2]. We have demonstrated that UCDMSCs cultured on honey-blended PVA substrate under standard condition decreases the ROS load. As the ROS load decreased, the fraction of senescent cells also decreased.

5 Conclusions

In this study, we have explored the consequences of culturing UCDMSC on electrospun PVA–honey nanofibre substrates to reduce their senescence in regenerative medicine applications. Incorporation of honey into the substrates exhibited antioxidant property, which could be observed up to day 5 indicating the release of antioxidant from the nanofibre membranes. Increased intracellular ROS load generated due to successive subculturing

was reduced by culturing UCDMSC on honey-loaded substrates. It can be concluded that honey incorporation played significant role in the reduction of ROS load in a passage-dependent manner. PVA–honey substrates were also effective in reducing senescence-associated changes of UCDMSC in a passage-dependent manner. From these complementary observations, the 0.5% honey concentration was considered optimum. Furthermore, these results suggested that the electrospun PVA–honey nanofibre membrane can be used as a suitable extracellular niche for the maintenance of UCDMSCs as well as used as a carrier for stem cell delivery in wound healing, regenerative medicine and tissue-engineering applications.

6 Acknowledgments

Financial & competing interests: AD was supported by the Institute scholarship from Indian Institute of Engineering Science and Technology, Shibpur. The authors acknowledge ICMR, Govt. of India for funding support.

7 References

[1] Forraz, N., McGuckin, C.P.: 'The umbilical cord: a rich and ethical stem cell source to advance regenerative medicine', *Cell Prolif.*, 2011, **44**, (Suppl 1), pp. 60–69

[2] Wagner, W., Horn, P., Castoldi, M., *et al.*: 'Replicative senescence of mesenchymal stem cells: a continuous and organized process', *PloS One*, 2008, **3**, pp. e2213–e2213

[3] Zhou, L., Chen, X., Liu, T., *et al.*: 'SIRT1-dependent anti-senescence effects of cell-deposited matrix on human umbilical cord mesenchymal stem cells', *J. Tissue Eng. Regen. Med.*, 2018, **12**, pp. e1008–e1021

[4] Cheng, H., Qiu, L., Ma, J., *et al.*: 'Replicative senescence of human bone marrow and umbilical cord derived mesenchymal stem cells and their differentiation to adipocytes and osteoblasts', *Mol. Biol. Rep.*, 2011, **38**, pp. 5161–5168

[5] Allen, N.D., Baird, D.M.: 'Telomere length maintenance in stem cell populations', *Biochim. Biophys.Acta (BBA) – Mol. Basis Disease*, 2009, **1792**, pp. 324–328

[6] Yang, C., Chen, Y., Li, F., *et al.*: 'The biological changes of umbilical cord mesenchymal stem cells in inflammatory environment induced by different cytokines', *Mol. Cell. Biochem.*, 2018, **446**, pp. 171–184

[7] Basciano, L., Nemos, C., Foliguet, B., *et al.*: 'Long term culture of mesenchymal stem cells in hypoxia promotes a genetic program maintaining their undifferentiated and multipotent status', *BMC Cell Biol.*, 2011, **12**, pp. 12–12

[8] Heo, J.-Y., Jing, K., Song, K.-S., *et al.*: 'Downregulation of APE1/ref-1 Is involved in the senescence of mesenchymal stem cells', *Stem Cells*, 2009, **27**, pp. 1455–1462

[9] Boopathy, A.V., Pendergrass, K.D., Che, P.L., *et al.*: 'Oxidative stress-induced Notch1 signaling promotes cardiogenic gene expression in mesenchymal stem cells', *Stem Cell. Res. Ther.*, 2013, **4**, pp. 43–43

[10] Gattazzo, F., Urciuolo, A., Bonaldo, P.: 'Extracellular matrix: a dynamic microenvironment for stem cell niche', *Biochim. Biophys. Acta*, 2014, **1840**, pp. 2506–2519

[11] Chai, C., Leong, K.W.: 'Biomaterials approach to expand and direct differentiation of stem cells', *Mol. Ther.*, 2007, **15**, pp. 467–480

[12] Bara, J.J., Richards, R.G., Alini, M., *et al.*: 'Concise review: bone marrow-derived mesenchymal stem cells change phenotype following In vitro culture: implications for basic research and the clinic', *Stem Cells*, 2014, **32**, pp. 1713–1723

[13] Hao, H., Chen, G., Liu, J., *et al.*: 'Culturing on wharton's jelly extract delays mesenchymal stem cell senescence through p53 and p16INK4a/pRb pathways', *PloS One*, 2013, **8**, pp. e58314–e58314

[14] Mohammadi, Z., Sharif Zak, M., Majdi, H., *et al.*: 'The effect of chrysin–curcumin-loaded nanofibres on the wound-healing process in male rats', *Artif. Cells Nanomed. Biotechnol.*, 2019, **47**, pp. 1642–1652

[15] Kornicka, K., Nawrocka, D., Lis-Bartos, A., *et al.*: 'Polyurethane–polylactide-based material doped with resveratrol decreases senescence and oxidative stress of adipose-derived mesenchymal stromal stem cell (ASCs)', *RSC Adv.*, 2017, **7**, pp. 24070–24084

[16] Pajoum Shariati, S.R., Shokrgozar, M.A., Vossoughi, M., *et al.*: 'In vitro Co-culture of human skin keratinocytes and fibroblasts on a biocompatible and biodegradable scaffold', *Iran Biomed. J.*, 2009, **13**, pp. 169–177

[17] Maleki, H., Gharehaghaji, A.A., Dijkstra, P.J.: 'A novel honey-based nanofibrous scaffold for wound dressing application', *J. Appl. Polym. Sci.*, 2013, **127**, pp. 4086–4092

[18] Eteraf-Oskouei, T., Najafi, M.: 'Traditional and modern uses of natural honey in human diseases: A review', *Iran J. Basic Med. Sci.*, 2013, **16**, pp. 731–742

[19] Sarkar, R., Ghosh, A., Barui, A., *et al.*: 'Repositing honey incorporated electrospun nanofiber membranes to provide anti-oxidant, anti-bacterial and anti-inflammatory microenvironment for wound regeneration', *J. Mater. Sci., Mater. Med.*, 2018, **29**, p. 31

[20] Dai, Z., Ronholm, J., Tian, Y., *et al.*: 'Sterilization techniques for biodegradable scaffolds in tissue engineering applications', *J. Tissue. Eng.*, 2016, **7**, pp. 2041731416648810–2041731416648810

[21] Mennan, C., Wright, K., Bhattacharjee, A., *et al.*: 'Isolation and characterisation of mesenchymal stem cells from different regions of the human umbilical cord', *BioMed Res. Int.*, 2013, **2013**, pp. 916136–916136

[22] da Rocha, R.G., Santos, E.M.S., Santos, E.M., *et al.*: 'Leptin impairs the therapeutic effect of ionizing radiation in oral squamous cell carcinoma cells', *J. Oral Pathol. Med.*, 2019, **48**, pp. 17–23

[23] Chakraborty, A., Das, A., Raha, S., *et al.*: 'Size-dependent apoptotic activity of gold nanoparticles on osteosarcoma cells correlated with SERS signal', *J. Photochem. Photobiol. B, Biol.*, 2020, **203**, p. 111778

[24] Kureel, S.K., Mogha, P., Khadpekar, A., *et al.*: 'Soft substrate maintains proliferative and adipogenic differentiation potential of human mesenchymal stem cells on long term expansion by delaying senescence', bioRxiv, 2018, p. 364059

[25] Younis, L.T., Abu Hassan, M.I., Taiyeb Ali, T.B., *et al.*: '3d TECA hydrogel reduces cellular senescence and enhances fibroblasts migration in wound healing', *Asian J. Pharm. Sci.*, 2018, **13**, pp. 317–325

[26] Kornicka, K., Nawrocka, D., Lis, A., *et al.*: 'Polyurethane–polylactide-based material doped with resveratrol decreases senescence and oxidative stress of adipose-derived mesenchymal stromal stem cell (ASCs)', 2017, **7**

[27] Qi, J., Zhang, H., Wang, Y., *et al.*: 'Development and blood compatibility assessment of electrospun polyvinyl alcohol blended with metallocene polyethylene and plectranthus amboinicus (PVA/mPE/PA) for bone tissue engineering', *Int. J. Nanomed.*, 2018, **13**, pp. 2777–2788

[28] Tunma, S., Inthanon, K., Chaiwong, C., *et al.*: 'Improving the attachment and proliferation of umbilical cord mesenchymal stem cells on modified polystyrene by nitrogen-containing plasma', *Cytotechnology*, 2013, **65**, pp. 119–134

[29] Anantharaju, P.G., Gowda, P.C., Vimalambike, M.G., *et al.*: 'An overview on the role of dietary phenolics for the treatment of cancers', *Nutr. J.*, 2016, **15**, pp. 99–99

[30] Chepulis, L.M., Buntting, C., Molan, P.: 'The effect of dilution on the rate of hydrogen peroxide production in honey and its implications for wound healing', *J. Altern. Complement. Med.*, 2003, **9**, pp. 267–273

[31] Minden-Birkenmaier, B.A., Bowlin, G.L.: 'Honey-based templates in wound healing and tissue engineering', *Bioeng. (Basel, Switzerland)*, 2018, **5**, p. 46

[32] Dominici, M., Le Blanc, K., Mueller, I., *et al.*: 'Minimal criteria for defining multipotent mesenchymal stromal cells. The international society for cellular therapy position statement', *Cytotherapy*, 2006, **8**, pp. 315–317

[33] Huang, C.-Y., Hu, K.-H., Wei, Z.-H.: 'Comparison of cell behavior on pva/pva-gelatin electrospun nanofibers with random and aligned configuration', *Sci. Rep.*, 2016, **6**, p. 37960

[34] You, S., Kublin, C.L., Avidan, O., *et al.*: 'Isolation and propagation of mesenchymal stem cells from the lacrimal gland', *Invest. Ophthalmol. Visual Sci.*, 2011, **52**, pp. 2087–2094

[35] Lisi, A., Briganti, E., Ledda, M., *et al.*: 'A combined synthetic-fibrin scaffold supports growth and cardiomyogenic commitment of human placental derived stem cells', *PloS One*, 2012, **7**, pp. e34284–e34284

[36] Corselli, M., Crisan, M., Murray, I.R., *et al.*: 'Identification of perivascular mesenchymal stromal/stem cells by flow cytometry', *Cytometry A*, 2013, **83A**, pp. 714–720

[37] Jeon, B.-G., Bharti, D., Lee, W.-J., *et al.*: ' comparison of mesenchymal stem cells isolated from various tissues of isogenic mini-pig', *Animal Cells Syst. (Seoul)*, 2015, **19**, pp. 407–416

[38] LeBert, D., Squirrell, J.M., Freisinger, C., *et al.*: 'Damage-induced reactive oxygen species regulate vimentin and dynamic collagen-based projections to mediate wound repair', *eLife*, 2018, **7**, p. e30703

[39] Lian, N., Wang, W., Li, L., *et al.*: 'Vimentin inhibits ATF4-mediated osteocalcin transcription and osteoblast differentiation', *J. Biol. Chem.*, 2009, **284**, pp. 30518–30525

[40] Ok, J.S., Song, S.B., Hwang, E.S.: 'Enhancement of replication and differentiation potential of human bone marrow stem cells by nicotinamide treatment', *Int. J. Stem Cells*, 2018, **11**, pp. 13–25

[41] Yang, S.-R., Park, J.-R., Kang, K.-S.: 'Reactive oxygen Species in mesenchymal stem cell aging: implication to lung diseases', *Oxid. Med. Cell. Longevity*, 2015, **2015**, pp. 486263–486263

[42] Zorov, D.B., Juhaszova, M., Sollott, S.J.: 'Mitochondrial reactive oxygen Species (ROS) and ROS-induced ROS release', *Physiol. Rev.*, 2014, **94**, pp. 909–950

[43] Denu, R.A., Hematti, P.: 'Effects of oxidative stress on mesenchymal stem cell biology', *Oxid. Med. Cell. Longevity*, 2016, **2016**, pp. 2989076–2989076

[44] Estrada, J.C., Torres, Y., Benguría, A., *et al.*: 'Human mesenchymal stem cell-replicative senescence and oxidative stress are closely linked to aneuploidy', *Cell Death Dis.*, 2013, **4**, pp. e691–e691

[45] Malone, M., Tsai, G.: 'Wound healing with apitherapy: A review of the effects of honey', *J. Apitherapy*, 2016, **1**, pp. 29–32

[46] Majtan, J.: 'Methylglyoxal-a potential risk factor of manuka honey in healing of diabetic ulcers', *Evid. Based Complement Alternat. Med.*, 2011, **2011**, pp. 295494–295494

[47] Hadagali, M.D., Chua, L.S.: 'The anti-inflammatory and wound healing properties of honey', *Eur. Food Res. Technol.*, 2014, **239**, pp. 1003–1014

[48] Brandl, A., Meyer, M., Bechmann, V., *et al.*: 'Oxidative stress induces senescence in human mesenchymal stem cells', *Exp. Cell Res.*, 2011, **317**, pp. 1541–1547

[49] Patlevič, P., Vašková, J., Švorc, P.Jr., *et al.*: 'Reactive oxygen species and antioxidant defense in human gastrointestinal diseases', *Integrative Med. Res.*, 2016, **5**, pp. 250–258

[50] Niccoli, T., Partridge, L.: 'Ageing as a risk factor for disease', *Curr. Biol.*, 2012, **22**, pp. R741–R752

[51] Kurutas, E.B.: 'The importance of antioxidants which play the role in cellular response against oxidative/nitrosative stress: current state', *Nutr. J.*, 2016, **15**, p. 71

[52] Correia-Melo, C., Passos, J.F.: 'Mitochondria: are they causal players in cellular senescence?', *Biochim. Biophys. Acta (BBA) – Bioenerg.*, 2015, **1847**, pp. 1373–1379
[53] Ziegler, D.V., Wiley, C.D., Velarde, M.C.: 'Mitochondrial effectors of cellular senescence: beyond the free radical theory of aging', *Aging Cell*, 2015, **14**, pp. 1–7
[54] Stanković, N., Mihajilov-Krstev, T., Zlatković, B.*, et al.*: 'Antibacterial and antioxidant activity of traditional medicinal plants from the Balkan Peninsula', *NJAS – Wageningen J. Life Sci.*, 2016, **78**, pp. 21–28
[55] Hixon, K.R., Lu, T., McBride-Gagyi, S.H.*, et al.*: 'A comparison of tissue engineering scaffolds incorporated with manuka honey of varying UMF', *BioMed Res. Int.*, 2017, **2017**, pp. 4843065–4843065
[56] Balikov, D.A., Crowder, S.W., Lee, J.B.*, et al.*: 'Aging donor-derived human mesenchymal stem cells exhibit reduced reactive oxygen Species loads and increased differentiation potential following serial expansion on a PEG-PCL copolymer substrate', *Int. J. Mol. Sci.*, 2018, **19**, p. 359
[57] Tan, J.J., Azmi, S.M., Yong, Y.K.*, et al.*: 'Tualang honey improves human corneal epithelial progenitor cell migration and cellular resistance to oxidative stress in vitro', *PloS One*, 2014, **9**, pp. e96800–e96800